Materials Science and Technology

ISSN: 0267-0836 (Print) 1743-2847 (Online) Journal homepage: https://www.tandfonline.com/loi/ymst20

Prediction of creep life of X10CrMoVNbN-91 (P-91) steel through short term stress relaxation test methodology

S.C. Bose, Kulvir Singh, J. Swaminathan & D.S. Sarma

To cite this article: S.C. Bose, Kulvir Singh, J. Swaminathan & D.S. Sarma (2004) Prediction of creep life of X10CrMoVNbN-91 (P-91) steel through short term stress relaxation test methodology, Materials Science and Technology, 20:10, 1290-1296, DOI: 10.1179/026708304225022304

To link to this article: https://doi.org/10.1179/026708304225022304

Published online: 19 Jul 2013.

Submit your article to this journal

Article views: 156

View related articles

Citing articles: 1 View citing articles

Full Terms & Conditions of access and use can be found at
https://www.tandfonline.com/action/journalInformation?journalCode=ymst20

Prediction of creep life of X10CrMoVNbN-91 (P-91) steel through short term stress relaxation test methodology

S. C. Bose, Kulvir Singh, J. Swaminathan and D. S. Sarma

The methodology proposed here adopts short-term stress relaxation testing (SRT) to predict creep strength/life of X10CrMoVNbN 91 (P-91) steel. SRT has been performed at three temperatures (853, 873, 898 K), and at each temperature two prestrains (0·7 and 1·2%) were applied with a hold time of 7 h. The initial data, stress versus time, were converted to stress versus inelastic strain rate by computation and compared with conventional steady state creep rate. Creep life was predicted from the SRT results using the Monkman–Grant relationship, and compared with creep data. The comparison showed the predicted life to agree extremely well with the creep-rupture life ($\approx$30 000 h). The calculated activation energy for SRT (719 kJ mol^{-1}) was found to be higher than the creep (415 kJ mol^{-1}). Detailed SEM and TEM studies revealed that the degradation of microstructure in terms of coarsening of $M_{23}C_6$, and martensitic lath grains, had taken place and was commensurable to long term creep exposure. MST/5907

Keywords: P-91 steel, Ferritic–martensitic steel, Stress relaxation, Creep, Microstructure

Mr Bose and Mr Kulvir Singh are in the Metallurgy Department, Corporate R&D, BHEL, Hyderabad 500093, India (samir@bhelrnd.co.in). Dr Swaminathan is in the MST Division, National Metallurgical Laboratory, Jamshedpur 831007, India, and Professor Sarma is in the Department of Metallurgy, Banaras Hindu University, Varanasi 221005. India. *Manuscript received 1 July 2003; accepted 9 June 2004.*
© 2004 Institute of Materials, Minerals and Mining. Published by Maney on behalf of the Institute.

Introduction

Metals and alloys operating at high temperature are usually characterised either by their creep strength (minimum creep rate) or stress rupture strength (time to fracture) at design stress and temperature. To measure reliability and to provide accurate long term prediction, regulatory bodies such as ISO, ASME, Indian Boiler Board etc., recommend conducting creep rupture tests up to around one third of the design life (usually 100 000 h). To meet the requirement, a large number of creep tests are performed, generally at three temperatures (service temperature and service temperature $\pm$25°C) and five stress levels, taking two specimens at each condition and from three heats. Thus, to satisfy the programme, around 90 specimens are required, taking around 4 years, a large number of creep test machines, high energy consumption and use of manpower. However, the irony is that even after accumulation of this huge amount of test data, extrapolation to the design life is found to be inaccurate.[1] Further, to qualify a material for (say) cast dependency of creep properties, short term 'go'–'no-go' tests are performed at stresses and temperatures well above the design values to obtain rupture lives of around 100–200 h. For acceptance criterion, the result should fall within a $\pm$20% scatter band of the 'master curve' of the material. The validity of this approach may be questionable since with the isothermal technique of conventional creep testing, transitions in deformation mechanism affecting rupture lives occur when loading stresses are applied below the Orowan bowing stress ($\approx$half of the yield stress) giving rise to a sigmoidal shape of stress versus rupture life curve.

The proposed short term stress relaxation test (SRT), though primarily carried out to determine the relaxation strength of bolt material for high temperature applications,[2] contains all the attributes of creep deformation. Stress relaxation occurs because of an exchange of elastic strain with a time dependent inelastic strain. The physical quantities derived from the SRT curves are the relaxed stress and change of stress rate as a function of time; both of these parameters are actually governed by inelastic strain rate during relaxation.[3] As the methodology is self programmed and has the capacity to deliver a wide range of strain rates (10^{-1} to 10^{-7} h^{-1}) in a single run within a short span of time, it can be exploited to determine creep strength as well as life of metals and alloys. The inelastic strain rates generated are comparable with steady state creep rates, albeit derived through a different deformation path[4,5]

Usually, raw stress–time data is converted to stress–plastic strain rate by using a simple mathematical derivation. As the elastic strain ε_e is proportional to the stress σ within the proportional limit zone, the elastic strain rate is given by

$$\dot{\varepsilon} = 1/E \times d\sigma/dt \quad \ldots\ldots\ldots\ldots (1)$$

where E is Young's modulus.

In pure stress relaxation, the sum of elastic strain ε_e and plastic strain ε_p is constant

$$\varepsilon_e + \varepsilon_p = \varepsilon_T = \text{constant} \quad \ldots\ldots\ldots\ldots (2)$$

Differentiating equation (2) with respect to time t and substituting the value of elastic strain rate f_e in equation (1) and rearranging, the plastic strain rate f_p can be deduced as

$$\dot{\varepsilon}_p = -1/E \times d\sigma/dt \quad \ldots\ldots\ldots\ldots (3)$$

where E is Young's modulus and σ is applied stress.

In recent decades, active development and evaluation of ferritic–martensitic steels with improved creep strength has been carried out to achieve higher operating temperatures and pressures and to minimise pollution in fossil power plants.[6,7] In view of this, a modified version of 9Cr1Mo with Nb stabilisation (X10CrMoVNbN 91) was developed in the USA and became accepted worldwide, appearing in US, UK, German, and Draft European specifications or data sheets. In boilers in many types of power plant, low alloy steel variants are gradually being replaced with this new grade of modified high Cr ferritic–martensitic steel. In

 DOI 10.1179/026708304225022304

Table 1 Chemical composition of P-91 boiler grade steel

Source	C	Si	Mn	P	S	Cr	Mo	V	Nb	N	Ni	Al
AR P-91	0·09	0·40	0·43	0·015	<0·01	8·80	0·89	0·19	0·10	0·05	0·09	0·024
P/T–91	0·08–0·12	0·20–0·50	0·03–0·60	0·02	0·01	8·0–9·5	0·85–1·05	0·18–0·25	0·06–0·10	0·03–0·01	0·40	0·04
ASTM				max	max						max	

India too, this same grade of material has been used in high pressure boilers since 1990.

The specific objective of the present work is to propose a short term stress relaxation test (SRT) methodology to predict long term creep strength/rupture life of a boiler grade X10CrMoVNbN 91 steel, popularly known as P/T–91 steel. An assessment of the microstructural changes is attempted with the help of light optical microscopy (LOM), scanning electron microscopy (SEM) and transmission electron microscopy (TEM) after SRT, and a comparison with long term creep exposure is made.

Experimental procedures

X10CrMoVNbN 91, popularly known as P/T–91 boiler grade steel, was selected for the current experiment. ASTM/ASME approved the material in 1983, designating it as A 335 P91, included in ASME section VIII and I. The steel will be referred to as AR P-91for this current work. The detail chemical composition of the sample AR P-91 steel is shown in Table 1, and was found to conform to the ASTM specification. The sample material was received in pipe form (320 mm outside diameter (OD) $\times$28 mm thickness), having been subjected to the following heat treatment cycles prior to dispatch. Normalised at 1323 K$\pm$ 283 K for 1 h followed by air cooling and tempering at 1013 K$\pm$283 K for 2 h followed by air cooling. The as received microstructure of AR P-91 steel is, therefore, fine grained tempered martensite type.

STRESS RELAXATION TEST

The SRT was carried out under close loop strain control mode using an Instron model 8562, 100 kN capacity electromechanical universal test machine, interfaced with an 8500 digital controller. Test control and data acquisition were done through MAX software supplied with the machine. The strain was controlled to within $\pm$1·0% of the set value. Strain measurements were monitored through a high temperature extensometer. A cylindrical type specimen was used with an effective gauge length GL of 12·5 mm and 6·5 mm diameter. The temperature was monitored using two Pt–Pt+13%Rh thermocouples tied along the GL of the specimen and continuously monitored and maintained within $\pm$274·5 K of the set value using a three zone wound furnace fitted with Eurotherm temperature controllers. The initially applied plastic strains (%) were preprogrammed and fast loading, at a strain rate of 0·01% s^{-1}, was applied. On achieving the requisite strain (%), the crosshead was locked or held constant and the specimen allowed to relax. All tests were run for 7 h. The initial raw data, stress versus time, was converted into stress versus strain rate using equation (3) through computer software.

HARDNESS MEASUREMENT

Room temperature Viskers hardness measurements HV(30 kg) were conducted on gauge portions of stress relaxation tested samples for all conditions and on a few crept samples tested at 873 and 898 K under low stress and also on AR P-91 steels. The results are shown in Table 2.

METALLOGRAPHY

Metallographic studies were carried out on specimens of AR P-91 material, crept specimens (100 MPa/898 K/4292 h) and stress relaxed specimens tested at 898 K and 1·2% prestrain (SR-6), using LOM, SEM, and TEM. SEM-EDX analyses were made on carbide/inclusion particles to identify the qualitative composition based on X-ray peak intensities of specific elements. Thin foils for TEM studies were prepared by a conventional technique and were observed using a JEOL 200 CX microscope operating at 160 kV. Except for AR P-91 steel, thin foil coupons for SRT and creep ruptured specimens were prepared from the gauge portion of samples and parallel to the stress axis. TEM microstructural characterisation utilised bright field and dark field microscopy and selected area diffraction patterns (SAD). The growth of the carbides was estimated by measuring the minor axis of the elliptical carbide particles ($M_{23}C_6$), and the growth of martensitic lath grains were estimated by measuring the width at various locations. The average values are listed in Table 3. The resultant microstructure after SRT was compared with the crept samples tested at identical test temperatures.

Results

The SRT was conducted at 853, 873 and 898 K and at each temperature, two prestrains, 0·7 and 1·2%, were applied for 7 h. Figure 1 shows a representative plot of stress versus relaxation time (in minutes) of specimens prestrained to

Table 2 Hardness measurements on stress relaxation and creep rupture tested samples of P-91 steel

Sample code	Test method	Test condition – SRT (%strain/temp K)	Test condition – creep stress, MPa/temp. K/life, h	Average hardness HV(30)
AR P-91	As received	–	–	224
SR-1	SRT	0·7/853	–	217
SR-2	SRT	1·2/853	–	215
SR-3	SRT	0·7/873	–	212
SR-4	SRT	1·2/873	–	210
SR-5	SRT	0·7/898	–	209
SR-6	SRT	1·2/898	–	206
Ref. 8 P-91	As received	–	–	224
	Creep	–	120/873/4641	200
	Creep	–	98/898/4292	204
Ref. 13 P-91	As received	–	–	230
	Creep	–	LMP=20 000$\approx$2500 h at 898 K	200
	Creep	–	LMP=21 500$\approx$10 000 h at 898 K	190

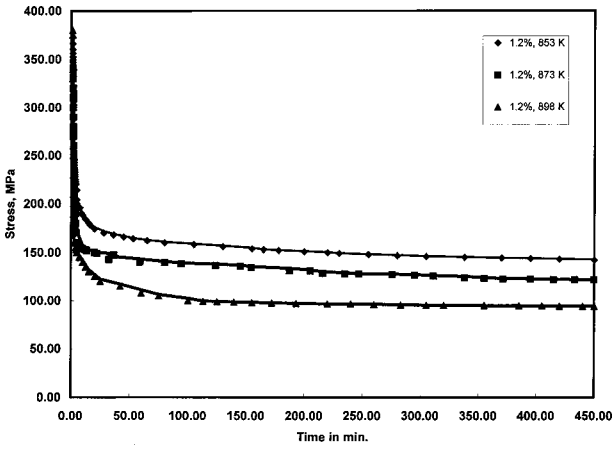

1 Stress relaxation response of AR P-91 steel at 1·2% plastic strain at 853, 873, and 898 K

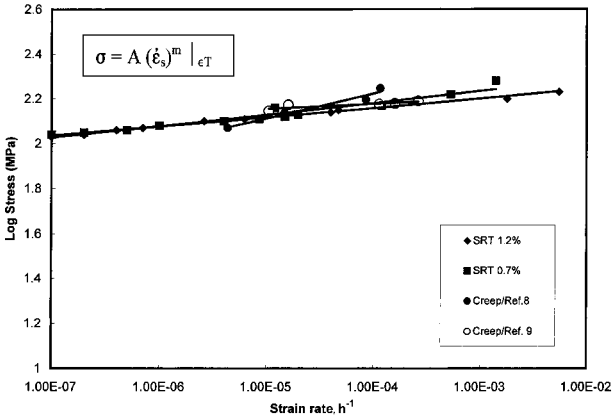

2 Comparison of creep strain rate behaviour obtained through SRT and conventional creep testing at 873 K

1·2% at all selected temperatures. Results for the SRT for a tension hold time of 7 h show a rapid drop in load/stress at the start of the hold time (Fig. 1), followed by a very gradual decrease in stress with time. The observed behaviour was the same for both increased test temperature, and for increased levels of applied strain (0·7−1·2%) at a specific test temperature. When computing inelastic strain rates from the raw data using Excel software on equation (3), it was observed that seven point numerical differentiation provided the best results. The estimated inelastic strain rates were then plotted against log of stress as shown in Figs 2 and 3 for 0·7% and 1·2% prestrains at 873 and 898 K respectively. In this study only the steady state region, i.e. 200 MPa stress (with corresponding strain rate 1×10^{-2} h^{-1}) and below were considered and compared with conventional steady state creep rate data[8–10] (note: the estimated strain rates for 853 K are not included in the plot due to the absence of comparison creep data). A

Table 3 Growth of $M_{23}C_6$ carbide (in diameter) and martensite lath width in as received, stress relaxed and crept P-91 steel

	Dimension in nm		
	$M_{23}C_6$(dia.)		
Sample code	GB	LB	Martensite lath (width)
AR P-91	124	102	540
SR–6 (1·2%, 898 K)	235	205	782
Creep (98/898 K/4292 h)	255	215	900

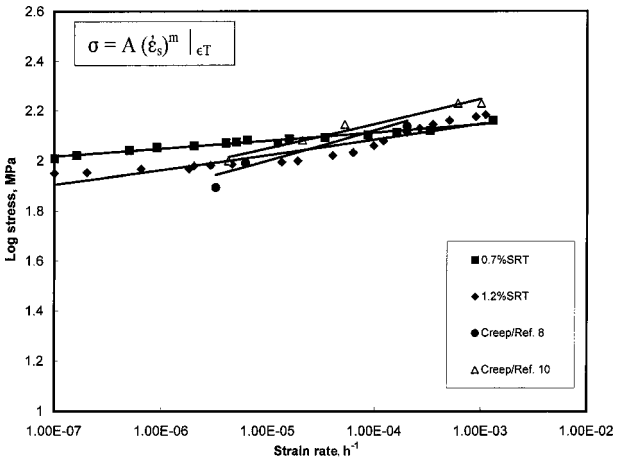

3 Comparison of creep strain rate behaviour obtained through SRT and conventional creep testing at 898 K

power law based model was used for best fitting of the curve. Over the 7 h test period, the inelastic strain rates obtained were in the range $5-8\times10^{-6}$ h^{-1}. The strain rates were extrapolated to a strain rate of 1×10^{-7} h^{-1} by a least squares regression model $\log y=\log a+m\log x$.

Creep rupture life was estimated from the calculated inelastic strain rates by applying the Monkman–Grant[11] relationship $\dot{\varepsilon}_s\times t_r^{m'}=C$, or $C/\dot{\varepsilon}_s=t_r^{m'}$ where, $\dot{\varepsilon}_s$ is the steady state creep rate, t_r is the rupture time and C and m' are constants). The constant $C=0{\cdot}02$ was taken from the work of Singh *et al.*[8] Figure 4 compares the rupture time t_r as a function of strain rate $\dot{\varepsilon}_p$ estimated at all test temperatures and 1·2% prestrain with conventional creep data. A power law regression model was fitted to the plot and an excellent fit ($R^2=1$) was obtained with $C=0{\cdot}02$ and $m'=1$. The predicted rupture lives at 873 and 898 K are plotted against original stresses in Figs 5 and 6 respectively, and compared with actual creep rupture data.[8–10,12] All predicted SRT rupture data were then fitted using the Larsen–Miller Parametric (LMP) equation and parametric values are plotted against stresses in Fig. 7 and compared with conventional creep test results.[8–10,12] The activation energy Q_c for both SRT and the creep test was estimated from the gradient $(-Q_c/R)$ of a plot of log $\dot{\varepsilon}_s$ versus log $1/T$ at a constant stress. The magnitude of Q_c based on stress relaxation and on creep for steel P-91 was 719 kJ mol^{-1} and 415 kJ mol^{-1}, respectively. Figure 8 shows a plot of the correlation between stress and temperature dependence of strain rate represented in terms of the estimated activation energy Q_c. A linear fit to the multilinear points was made using a stress exponent $n=11{\cdot}47$ and constant $B=-66{\cdot}0$.

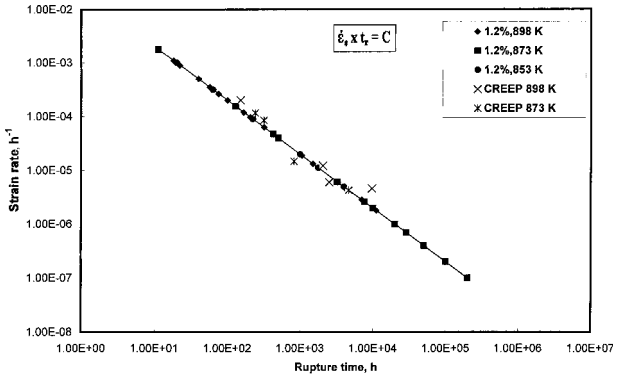

4 Monkman–Grant relationship of SRT data at 853, 873, and 898 K superimposed with creep data at 873 and 898 K for P-91 steel

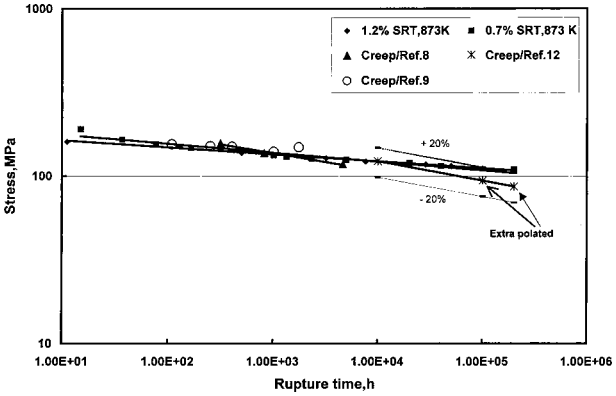

5 Comparison of predicted rupture life estimated using SRT with conventional creep rupture lives at 873 K for P-91 steel

Hardness measurements on SRT samples (Table 2) showed a steady decrease in hardness value with increasing test temperature and increasing prestrain. Table 2 also contains some hardness data for creep ruptured P-91 samples.[8,13] Note that the hardness of crept and SRT specimens at 898 K are comparable.

The starting microstructure of AR P-91 steel was tempered martensitic type (Fig. 9*a*) with a fine distribution of dominant carbide of $M_{23}C_6$ precipitated at grain boundaries (GB) and lath boundaries. The average diameter of the carbides taken at the minor axis is documented in Table 3. Similarly, the martensite lath widths were measured under all test conditions, and the average values are shown in Table 3. Figures 9*a*–*c* show bright field TEM images comparing microstructural degradation, such as coarsening of $M_{23}C_6$ carbides, dispersion of particles, dislocation density etc. caused by SRT (Fig. 9*b*) and creep (Fig. 9*c*) for AR P-91 steel. Figure 10 shows TEM bright field images comparing only the martensitic lath structure and its coarsening as a result of SRT and creep at 898 K for P-91 material. The evidence of alloy carbide ($M_{23}C_6$) shearing due to the SRT deformation mechanism at higher prestrains (1·2%) at temperature 898 K is shown in the dark field TEM image of Fig. 11. Evidence of GB migration and sliding due to SRT deformation at 1·2% prestrain and 898 K is shown in Fig. 12.

Discussion

The response of initial plastic strain (%) in the form of flow stress curves (stress versus inelastic strain rate) has previously been studied in detail,[14,15] and it was shown that

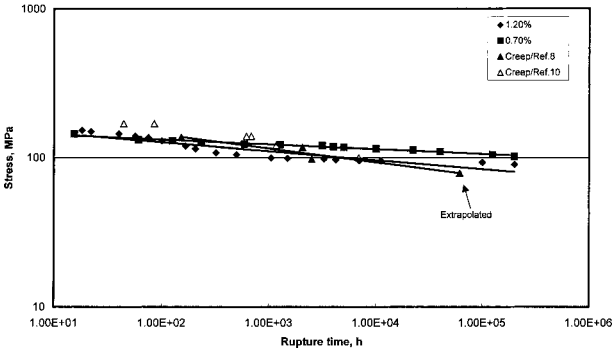

6 Comparison of predicted rupture life estimated using SRT with conventional creep rupture lives at 898 K for P-91 steel

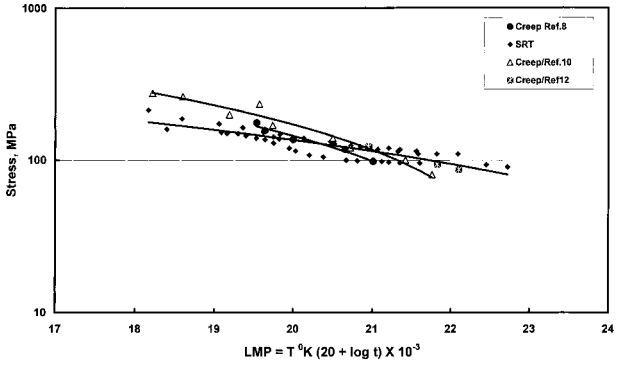

7 Comparison of stress versus LMP plots obtained using SRT and conventional creep for P-91 steel

initial plastic strain in excess of 0·5% could induce sufficient strain rate sensitivity into the matrix to be compatible with creep deformation. Further, it was observed that the higher the temperature and preplastic strain, the better the correlation with creep life.[15] Zamaric and Davis[16] commented that the rate of creep strain accumulation at $\Delta\varepsilon_t = 0{\cdot}5\%$ plastic strain is less than that at $\Delta\varepsilon_t = 1{\cdot}0\%$. Thus, the creep strain accumulation at $\Delta\varepsilon_t = 0{\cdot}5\%$ would be more indicative of low stress–long term creep compared to the higher creep strain accumulation at $\Delta\varepsilon_t = 1{\cdot}0\%$. This implies that the magnitude of initial work hardening plays a dominant role in deformation rate as it introduces greater dislocation density into the matrix.[17] Under the influence of a sustained test temperature and higher dynamic recovery rate constant, these dislocation arrays rapidly polygonise into subcells (dynamic recovery). The phenomenon introduces matrix softening, which is demonstrated by the drop in hardness (Table 2) to values comparable with crept material.[8] Kimura *et al.*[13] correlated the drop in hardness with LMP values for mod. 9Cr1Mo steel evaluated via a series of creep tests. The hardness drop corresponding to 2500–10 000 h (LMP = 20 000–21 500) was recorded as 200 HV(10) to 190 HV(10) at 898 K respectively (Table 2), which are slightly lower than the observed value (206 HV(30) at 898 K) obtained in the current experiment. This grade of steel has a tendency to demonstrate rapid inflexion of the creep rupture strength and hardness properties at lower stresses ($\approx$130 MPa) and at around 10 000 h at 898 K due to the structural deterioration and/or appearances of other phases.[13,18] It may be noted that in practice, a 7 h hold in SRT yielded an inelastic strain rate in the region of 5×10^{-6} h^{-1}, which is $\cong$4000 h of creep life (using the M–G relationship). Therefore, the structural softening introduced by SRT, particularly at higher

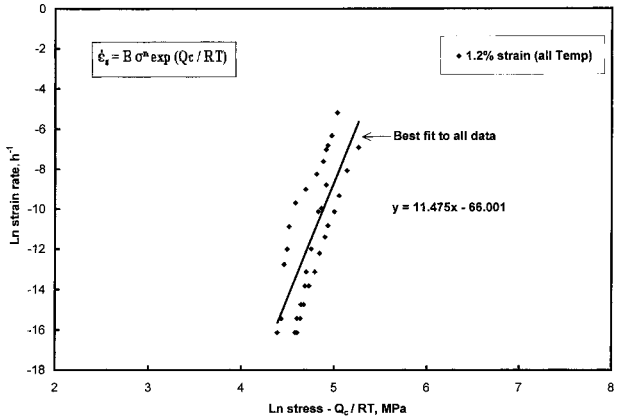

8 Temperature dependence of creep rate obtained using SRT, represented in terms of creep activation energy

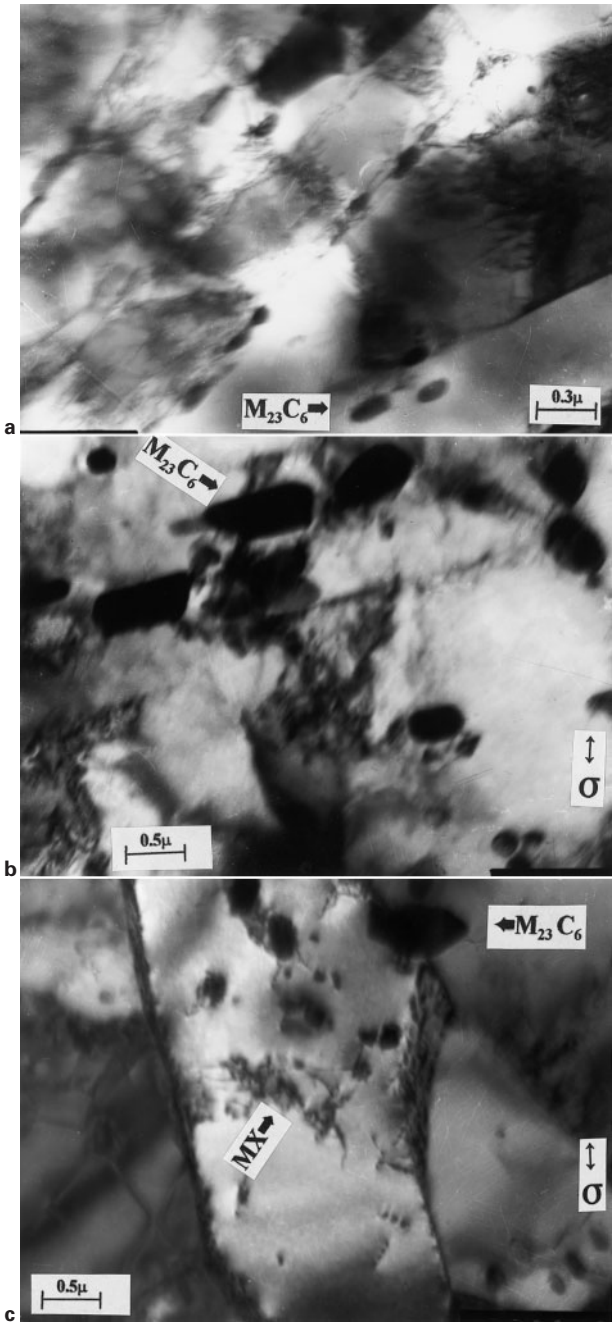

a as received; *b* SRT at 1·2% strain, 898 K; *c* crept at 98 MPa/898 K/4292 h

9 TEM bright field images comparing coarsening of $M_{23}C_6$ carbide and degradation of microstructure for P-91 steel under different conditions

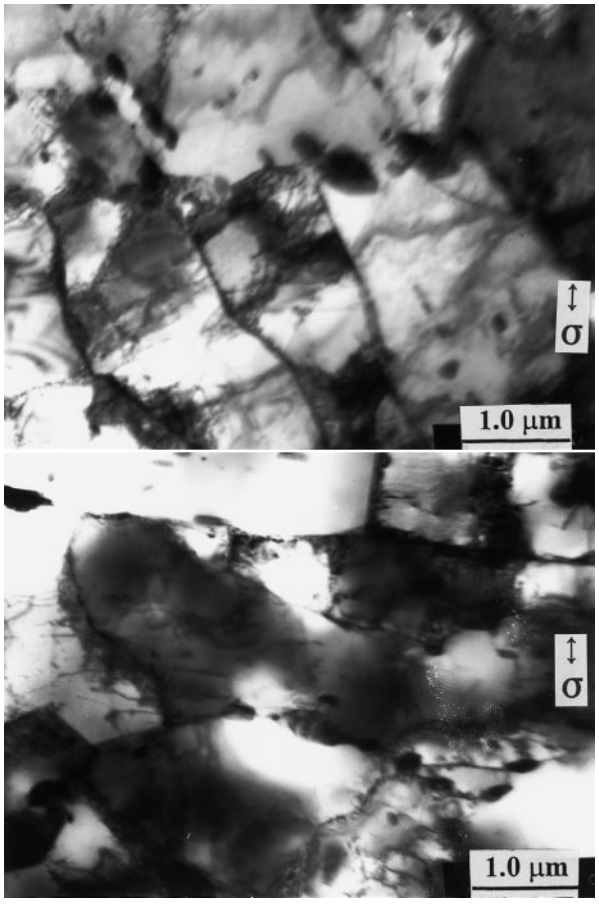

a SRT at 1·2% strain, 898 K; *b* crept at 98 MPa/898 K/4292 h

10 TEM bright field images comparing exclusively martensitic lath width, intralath recovery of dislocation, and dispersion of alloy carbides for P-91 steel under different conditions

temperature and prestrains compares well with the crept material.

Using equation (3), the rate of reducing stresses was converted into inelastic strain rates. The estimated strain rates are shown in Figs 2 and 3 for 873 K and 898 K respectively. A power law formulation has been used to model the strain rate $\dot{\varepsilon}_p$ dependency on stress σ in terms of strain rate sensitivity m at a constant strain ε and temperature T:

$$\sigma = A(\dot{\varepsilon}_p)^m|_{\varepsilon T} \quad \ldots\ldots\ldots\ldots\ldots\ldots \quad (4)$$

where A and m are constants and exponent m is known as the strain rate sensitivity and is given by $\log \sigma / \log \dot{\varepsilon}_p$.

The superimposed conventional creep strain rate data in Figs 2 and 3 show that there is close agreement between the strain rates determined by the two methodologies, indicating that physical quantities evaluated through both methodologies have the same meaning. The observation supports the proposals of Rohde and Swerengen[5] that the power law exponent n in stress relaxation is nearly equal to that for steady-state creep n'. Laflen and Jaske[19] examined the effect of load path and history on 2·25Cr1Mo low alloy steel and 304 and 316 stainless steel. They have shown that prediction of creep life from SRT data is achievable.

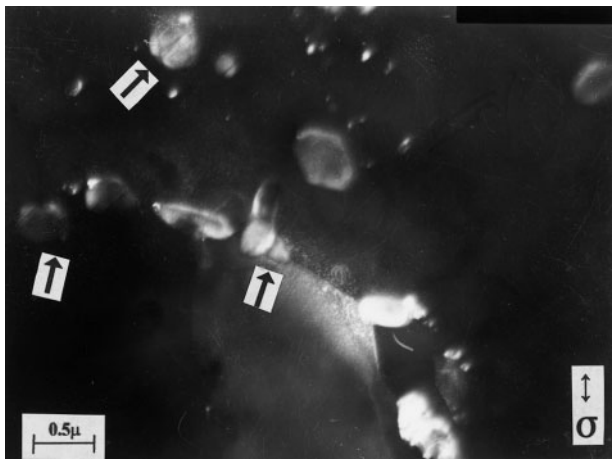

11 TEM dark field image showing shearing of $M_{23}C_6$ carbides (marked →) for SRT at 1·2% strain and 898 K

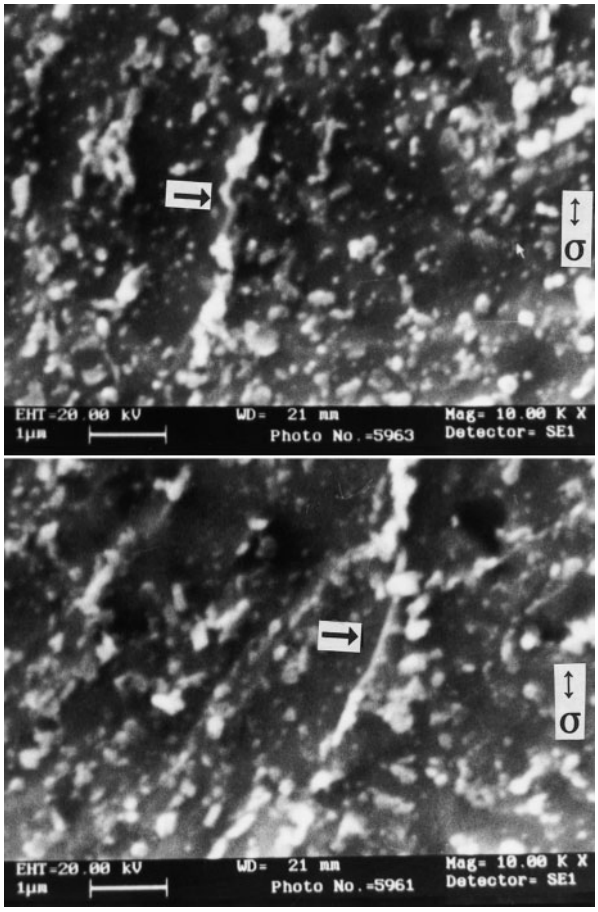

12 SEM micrograph showing *a* GB sliding (→) and *b* GB migration (→) in SRT sample. Test condition: 1·2% prestrain at 898 K. Note: alloy carbide appears as a white particulate against the background of dark gray ferrite

ESTIMATION OF RUPTURE LIFE

Of the many empirical relationships proposed to analyse the data, one that is most prominent and simple in application is that originally proposed by Monkman and Grant (M–G). The relationship between minimum creep rate and rupture time is regarded as evidence that the controlling mechanisms for deformation and fracture are essentially the same. The minimum creep rate used in the M–G relationship usually takes an average value of the steady state creep rate ε_s. Using the M–G relationship, the predicted rupture life through SRT when plotted against inelastic strain rate (Fig. 4), gave satisfactory confidence in the result. Its validation with conventional creep data justifies the methodology. A close comparison of predicted rupture lives with conventional creep rupture are shown in Figs 5 and 6 for 873 and 898 K. Figure 5 establishes well that the long term prediction of SRT data lies within the $\pm 20\%$ scatter band (limit for acceptance) of the long term conventional creep data evaluated by Kubon *et al.*[12] However, it was observed that SRT data at 898 K (Fig. 6) were in closer agreement than the results at 873 K. The LMP values of predicted rupture data at 853, 873, and 898 K are compared with other creep results[8,10,12] in Fig. 7. All these results emphatically show that with a hold time of around 7 h at the higher plastic strain (1·2%), the technique can estimate the rupture life up to $\approx 30\,000$ h quite accurately. Conventially, it would take tens of thousands of hours to achieve reliable life estimation.

The prediction of creep/creep rupture life has been attempted successfully in earlier experiments.[14,20] Woodford[14] concentrated mostly on the percentage creep life of materials rather than the rupture life, following the methodology proposed for creep data analysis by Goldhoff and Gill.[21] Daleo *et al.*,[20] on the other hand, estimated creep rupture life from SRT results on Ni based super alloys using an algorithm relating creep rate, fracture strain, and creep life. They obtained a band of rupture lives corresponding to different ranges of creep ductility.

Irrespective of the detailed mode of fracture, the creep characteristic of simple crystalline solids with a certain grain size are normally assessed by reference to the variation of secondary/minimum creep rate and its relation with stress, temperature, and rupture time, using a phenomenological equation of the form

$$1/t_r \propto \dot{\varepsilon}_s = B\,\sigma^n \exp^{(-Qc/RT)} \quad . \quad . \quad . \quad . \quad . \quad . \quad . \quad . \quad (5)$$

where t_r is rupture time, A and n are constants, Q_c is activation energy, and R is the universal gas constant. Equation (5) has recently been used to evaluate the activation energy and temperature compensated parameterised curves etc.[20,22] The stress and temperature dependence of creep rate represented in terms of activation energy for creep parameterised using equation (5) is shown in Fig. 8. The estimated apparent Q_c for creep (415 kJ mol^{-1}) is close to that of matrix self diffusion Q_{sd}, whereas for SRT ($Q_c = 719$ kJ mol^{-1}) it is much higher. The high Q_c in SRT is mainly ascribed to the large mobile dislocation density (activation volume V^*) created in the matrix during the loading to high initial plastic strain (%) before the start of relaxation, which introduces strain hardening into the matrix.[17] The phenomenon introduces arrays of mobile dislocation and they begin to serve as barriers to the glide motion of other dislocations. Further, the interactions of mobile dislocations with carbide particles situated at GBs, LBs, and within subgrain boundaries create a back stress or threshold stress, thus reducing the effective stress in the process. In a dynamic deformation such as SRT, to overcome these barriers or to detach particles from dislocations to a climb motion, a thermally activated process with high Q_c is required. Strudel[23] on Ni base super alloy (N–18), has shown Q_c to be higher at the initial stage of relaxation (high stress/strain rate region) and to reduce to a comparable level with creep as relaxation attained steady, i.e. at low stresses. At higher activated conditions, the mechanism of particle shearing by either single or paired matrix dislocations and/or the Orowan bowing dislocation mechanism are predominant. These are the general conditions for dislocation creep (dislocation glide aided by vacancy diffusion).[5,23–25] Therefore, a high degree of precipitate ripening[15,26] was assumed to take place at higher temperature, dominated by both high Q_c and n (stress exponent).

EVOLUTION OF MICROSTRUCTURE

Stress relaxation is often interpreted in terms of thermally activated deformation models and, therefore, some evolution of microstructure is normally expected. The current AR P-91 material is basically ferritic–martensitic type steel and offers excellent creep strength in the creep regime at 823–873 K. A detailed account of original microstructure and degeneration of microstructure due to creep exposure to various times is given elsewhere in the open literature for P/T–91 steel.[1,9,18,26] With the tempered martensite as base structure, strengthening is imparted by the fine distribution of $M_{23}C_6$ (Cr rich), M_2X (Cr rich), MX (Nb rich) and MC (V rich) carbides distributed along the GBs ($M_{23}C_6$), LBs ($M_{23}C_6$ and M_2X), and intralath matrix precipitation of MX and MC. $M_{23}C_6$ being the dominant carbide, its coarsening factor is important as far as creep resistance of the steel is concerned. The microstructural assessment of P-91 steel showed that the effect of 7 h hold time at 1·2%

prestrain/898 K had facilitated coarsening of $M_{23}C_6$ carbide from 124 nm to 235 nm at GBs and 102 nm to 205 nm at LBs (Table 3 and Fig. 9*b*). An average growth of 110 nm was recorded. In contrast, growth due to creep in an equivalent time was observed to be slightly more, $\approx$130 nm. The observed growth of carbide agrees well with other published results.[1,9,26] The observation establishes that with the SRT deformation mechanism, under high Q_c and stress exponent n, the Ostwald ripening of precipitated particles is accelerated.[15,26] The as received P-91 steel contained a high population of dislocation arrays within the lath martensite grains, 540 nm in width (Fig. 9*a*). After relaxation, considerable growth and recovery of tempered martensite microstructure, such as increase in lath width and subgrain size (Fig. 10*a*), was observed. The width of martensitic laths increased from 540 nm (as received) to 782 nm (after SRT) in comparison to the crept specimen ($\approx$900 nm), as shown in Figs 9*c* and 10*b*. The comparison establishes that significant progress in the recovery of martensitic substructure had taken place during the SRT process, comparable with conventional creep. This observation further supports the closeness of hardness values for both crept and stress relaxed samples at higher temperatures.

Evidence of particle shearing is shown in Fig. 11 (marked with arrows). The high Q_c and n (719 and 14 respectively) observed for the current steel has led to the suggestion that diffusion within the particles themselves could be an important phenomenon. In the regime of dislocation creep, deformation might have taken place as a result of a dislocation process occurring within the matrix or at the matrix/particle interface. Certainly, at high stress levels, the moving dislocation can cut the coherent particle.[25] Strudel[23] (SRT) and Guo *et al.*[24] (creep) have shown that particles like γ' (Ni_3 (Al,Ti)), were sheared under conditions of high Q_c and n.

A hold time of 7 h at 898 K and 1·2% prestrain caused a noticeable display of precipitate free zones (PFZ) at the vicinities of GBs (not presented here), GB sliding and its migration. Figure 12*a* and *b* respectively show the occurrence of GB sliding and its migration. The phenomenon is predominant at intermediate stresses. GB sliding is a result of GB dislocation motion and is frequently observed to be associated with GB migration.[27,28]. Due to the precipitation and growth of second phase particles at GBs, which eventually tried to restrict the sliding, the in between precipitate free regions were deformed and appeared as ledges (see the arrow in Fig. 12*a*). The inceptions of lateral GB migration (Fig. 12*b*) relaxed the shear stresses induced by GB sliding at the boundary regions. The observed GB migration is an indication of combined creep and plasticity, but mostly plasticity.

Conclusions

1. The result of short term SRT on P-91 steels is in very good agreement with the long-term creep results. For life determination it was observed that the testing at higher temperatures (898 K) and higher prestrain level (1·2%) yielded better correlation with the traditional creep rupture life.

2. The microstructural changes caused by SRT are very similar to those observed in specimens/components exposed to long term creep. The higher activation energy during SRT is attributed to be the cause for accelerating the microstructural degradation.

3. Life calculations are based on the Monkman–Grant relationship.

4. The agreement of short term SRT with long term creep test, both in terms of creep properties and associated microstructural changes, validates the technique for use as a laboratory tool during alloy development, for quality control and estimating the life of service exposed components.

Acknowledgements

The authors express their sincere thanks to Mr S. Balagurunathan, Executive Director (Corporate R&D, BHEL) for his encouragement and necessary permission for publication.

References

1. K. KIMURA, H. KUSHIMA and F. ABE: Proc. 5th Int. Conf. on 'Advanced materials for 21st century turbines and power plants', 3–7 July, (ed. A. Strang *et al.*), 590–602; 2000, London, The Institute of Materials.
2. ASM metals handbook, 10th edn, Vol. 8, 'Mechanical testing', 364; 2000, Materials Park, OH, ASM International.
3. A. A. ALY, T. G. ABDEL-MALIK, A. M. ABDEEN and H. M. ELABAMY: *Met. Sci. Eng.*, 1984, **62**, 181–185.
4. D. A. WOODFORD and K. IIJIMA: in 'Advances in turbine materials, design and manufacturing', (ed. A. Strang *et al.*), 613–624; 1997, London, The Institute of Materials.
5. R. W. ROHDE and J. C. SWEARENGEM: in 'Stress relaxation testing', (ed. A. Fox), STP 676, 21–35; 1978, Philadelphia, PA, ASTM.
6. D. A. CANINICO: 'Thick-walled pressure vessels for energy system. Technical programme and data package for use of modified 9Cr–1Mo steel', ASME Section I and VIII, April 1982.
7. V. K. SIKKA, C. T. WARD and K. C. THOMAS: Proc. Conf. 'Modified 9Cr–1Mo steel', October 1981, Warrendale, PA, 65–84.
8. KULVIR SINGH, S. C. BOSE and G. J. REDDY: 'Studies on creep rupture behaviour of weld joints of X10 CrMoNbN 91 and X20 CrMoV 12 1 steels'. Report no. RD: MTL: KS: 06:71, Corp. R&D, BHEL, 1999, India.
9. P. ANDERSON, T. BELLGARDT and F. L. JONES: *Mater. Sci. Technol.*, 2003, **19**, 207–213.
10. F. V. ELLIS and R. W. SWINDEMAN: *J. Press. Vess. Piping ASME*, 1993, **262**, 157–166.
11. F. C. MONKMAN and N. J. GRANT: *Proc. ASTM*, 1956, **56**, 593–605.
12. Z. KUBON, V. FOLDYNA, D. HAJDUK and P. SIMCEK: 'Parsons 2000: Advanced materials for 21st century turbines and power plant', (ed. A. Strang *et al.*), 485–497; 2000, London, IOM.
13. K. KIMURA, H. KUSHIMA, F. ABE, K. YAGI and H. IRIE: *Proc. 4th Int. Charles Persons Turbine Conference*',(ed. A. Strang *et al.*), 257–269; 1997, UK, IOM.
14. D. A. WOODFORD: *Mater. High Temp.*, 1997, **14**, 413–420.
15. S. C. BOSE, KULVIR SINGH and G. JAYARAMAN: *J. Test. Eval.*, 2003, **31**, (3), 183–195.
16. S. Y. ZAMARIK and D. C. DAVIS: *Trans. ASME*, 1991, **113**, 180–186.
17. A. K. GHOSH: *Acta Metall.*, 1980, **28**, 1443–1465.
18. A. STRANG, V. FOLDYNA, A. JACOBOVA, K. KUBON, V. VODAREK and J. LENERT: *Proc. 4th Int. Charles Parsons Turbine Conf.*, (ed. A. Strang *et al.*), 603–612; 1997, UK, IOM.
19. J. H. LAFLEN and C. E. JASKE: 'Stress relaxation testing', (ed. A. Fox), 182–205; 1978, ASTM STP 676.
20. J. A. DALEO, K. A. ELLISON and D. A. WOODFORD: *J. Eng. Gas Turbines Power*, 1999, **121**, 121–137.
21. R. M. GOLDHOFF and R. F. GILL: *Trans. ASME*, Paper no. 71 WA/Met-2, December 1971, pp. 1–6.
22. D. A. WOODFORD: Accelerated high temperature performance evaluation for alloy optimization, embrittlement and life assessment. MPa Inc. Santabarbara, CA 93101. Private Communication. 2001.
23. J. L. STRUDEL: in Proc. Int. Symp. on 'Materials ageing and life management', Vol. 2, (ed. Baldev Raj *et al.*), 649–656; 2000, New Delhi, Allied Publishers.
24. J. T. GUO, C. YUAN, H. C. YANG, V. LUPINC and M. MALDINI: *Metall. Mater. Trans. A*, 2001, **32A**, 1103–1110.
25. R. W. EVANS and B. WILSHIRE: 'Creep of metal and alloys', 1985, London, The Institute of Metals.
26. S. SPIGARELLI, E. CERRI, P. BIANCHI and E. EVANGELISTA: *Mater. Sci. Technol.*, 1999, **15**, 1433–1440.
27. A. HORSEWELL: *Scand. J. Metall.*, 1978, **7**, 36–37.
28. K. F. ASHBY: *Surf. Sci.*, 1972, **31**, 498–542.